

# Effect of some growth parameters on vacuum-deposited $\text{CuInSe}_2$ films

M. M. EL-NAHASS, H. S. SOLIMAN

*Faculty of Education, Ain Shams University, Heliopolis, Cairo, Egypt*

D. A. HENDI

*Girls' College of Education, Jeddah, Saudi Arabia*

KH. A. MADY

*Physics Department, National Research Centre, Dokki, Cairo, Egypt*

P-type copper indoselenide ( $\text{CuInSe}_2$ ) thin films were vacuum-deposited on glass substrates by a single-source thermal evaporation technique under different conditions of preparation. The structural properties of the films were investigated by X-ray diffraction and transmission electron microscopy and diffraction techniques. The dark resistivity of the deposited films was investigated as a function of film thickness, deposition rate and substrate temperature. The conductivity activation energy ranges from 0.851 to 1.01 eV depending on the deposition rate. Single-phase and stoichiometric  $\text{CuInSe}_2$  films could be deposited at low deposition rates (less than  $4 \text{ nm s}^{-1}$ ). Higher deposition rates led to multiphase films containing  $\text{InSe}$ ,  $\text{In}_2\text{Se}_3$ ,  $\text{CuSe}$  and  $\text{Cu}_3\text{Se}_2$  in addition to  $\text{CuInSe}_2$ .

## 1. Introduction

Copper indoselenide ( $\text{CuInSe}_2$ ) is one of the ternary semiconductors, which have attracted great interest due to their performance potential in photovoltaic and optoelectronic applications [1–4]. It crystallizes in the chalcopyrite structure. Depending on the conditions of the preparation,  $\text{CuInSe}_2$  films may be partially amorphous, polycrystalline or single-crystalline, and of a single-phase or multiphase form. Both *n*- and *p*-type polycrystalline films with a wide range of resistivity have been obtained [5–7]. Many methods for the preparation of  $\text{CuInSe}_2$  thin films were reported; for example, flash evaporation [8, 9], thermal evaporation using single-source, two-source or three-source techniques [10–12], radio-frequency sputtering [13] and spray pyrolysis [14].

Some structural characteristics of  $\text{CuInSe}_2$  films, prepared by single-source evaporation, have been reported [15–18] without referring to their dependence on the deposition rate.

We recently reported on the optical properties of  $\text{CuInSe}_2$  thin films [19] and the characteristics of *p*- $\text{CuInSe}_2$ -*n*- $\text{CdS}$  hetero-junctions [20]. The aim of the present work is to throw some light on the effect of the deposition rate and some other deposition parameters on the structural characteristics and the dark electrical resistivity of  $\text{CuInSe}_2$  films prepared by a single-source evaporation technique.

## 2. Experimental procedure

Polycrystalline ingots of  $\text{CuInSe}_2$  were initially prepared by direct fusion of the constituent elements in

the stoichiometric ratio in vacuum-sealed silica ampoules. A mixture of the resulting ingot and pure selenium was ground and heated in a vacuum-sealed silica ampoule for 15 min at 873 K [17]. The product was identified with X-ray diffraction to be  $\text{CuInSe}_2$  of the chalcopyrite structure, and to be *p*-type material as indicated by a hot probing technique. Thin films were prepared by a single-source thermal evaporation technique using a coating unit (Edwards 306A). Pre-cleaned glass substrates were fixed on a rotating holder at a height of 0.25 m above the evaporator (molybdenum boat) to obtain homogeneous films. Final cleaning of the substrate was achieved by ionic bombardment. The vacuum during deposition was kept at  $10^{-4}$  Pa. A precalibrated quartz crystal thickness monitor was used for controlling the film thickness and the deposition rate.

An X-ray diffractometer (Philips PW 1700) with Ni-filtered  $\text{CuK}_\alpha$ -radiation was used for X-ray diffraction (XRD) studies. Microstructural investigations were carried out using a transmission electron microscope (Jeol JEM 100 Cx).

The dark electrical resistivity was measured using a four-point probe technique with a square-array configuration (Fig. 1). The various corrections developed for such configuration were applied. The basic equation for the square array resting on the surface of a semi-infinite medium is [21]

$$\rho = 10.7 S \frac{V}{I}$$

where  $S$  is the side edge of the square. A high impedance ( $10^{14} \Omega$ ) electrometer (Keithley 616) was used

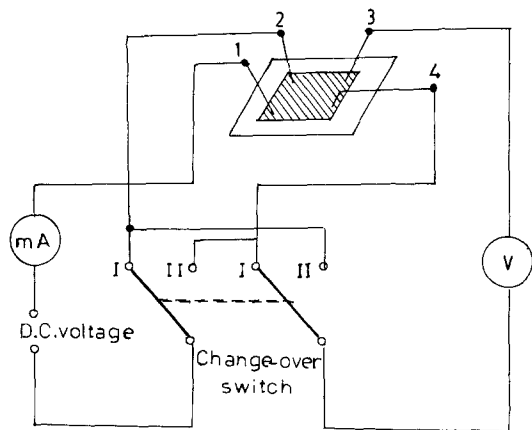


Figure 1 Schematic diagram of the four-point probe technique with a square-array configuration.

for measurements. The temperature of the specimen was determined by means of a Chromel–Alumel thermocouple.

### 3. Results and discussions

#### 3.1. Structural properties

Fig. 2 shows X-ray diffraction patterns of  $\text{CuInSe}_2$  films of the same thickness (500 nm) deposited on glass substrates with different deposition rates, compared with the powder pattern. The hot probing technique showed that the source material and the deposited films were *p*-type. At low deposition rates ( $0.1 \text{ nm s}^{-1}$ ) the pattern (Fig. 2a) corresponds to a single-phase  $\text{CuInSe}_2$  of the tetragonal system with preferred ori-

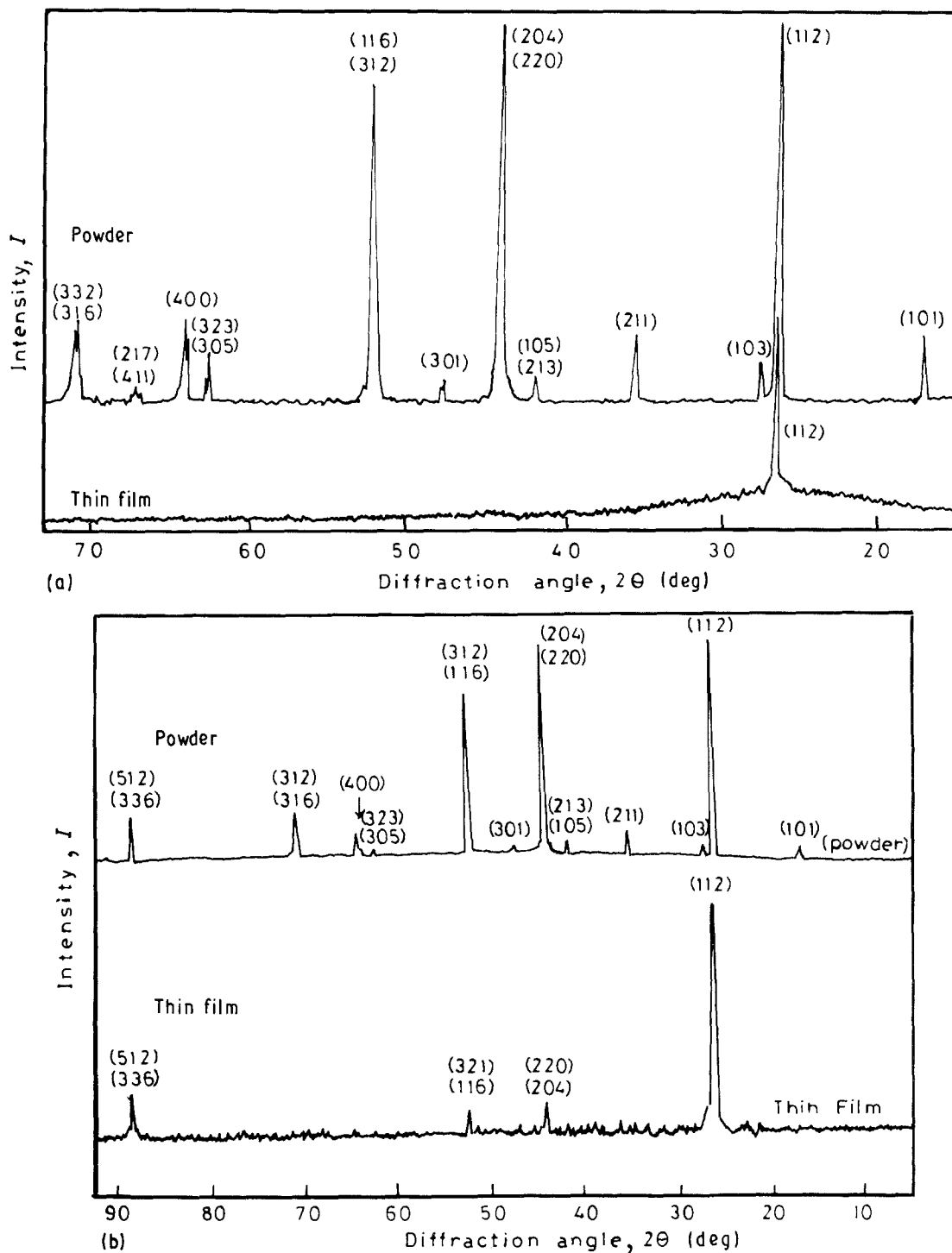


Figure 2

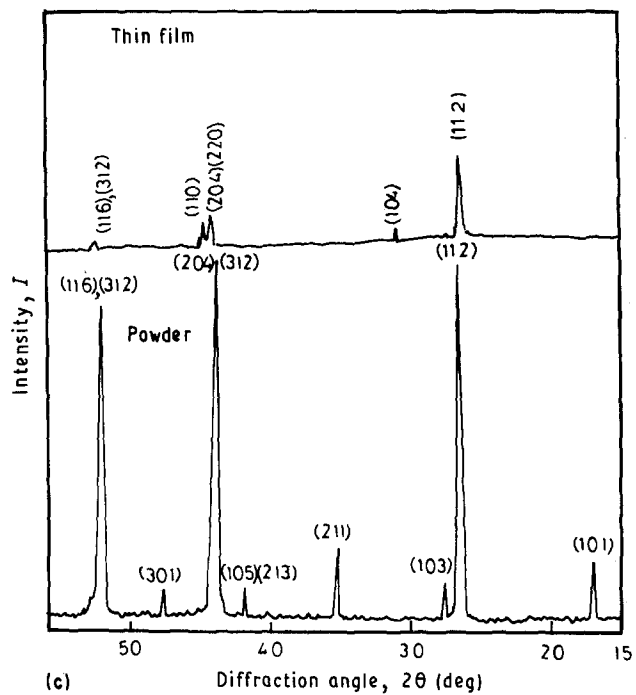


Figure 2 XRD patterns of  $\text{CuInSe}_2$  films of the same thickness (500 nm) deposited on glass substrates compared with the powder pattern. Deposition rate (a) 0.1, (b) 3.5 and (c)  $10 \text{ nm s}^{-1}$ .

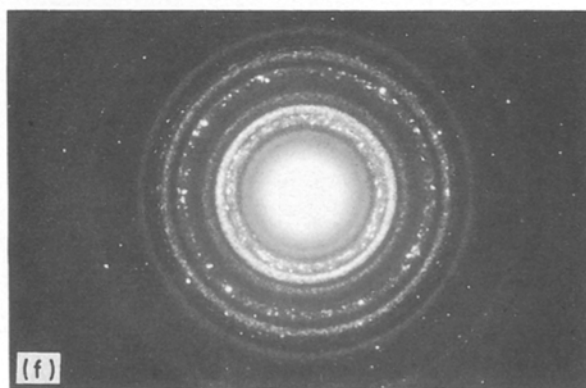
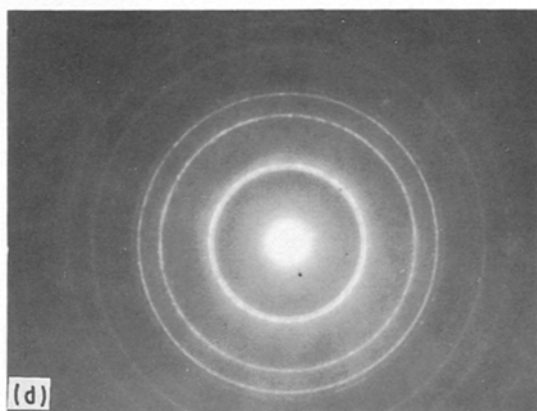
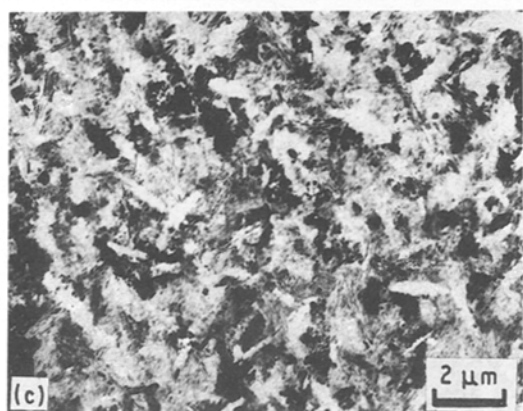
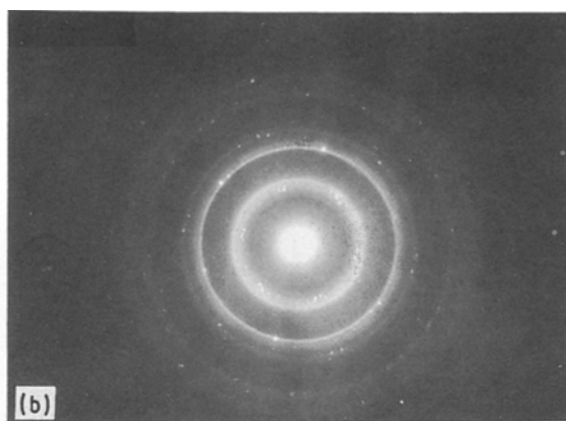
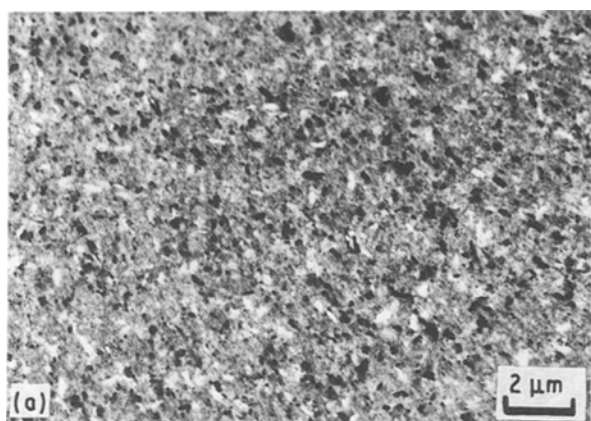


Figure 3 TEM micrographs and diffraction patterns of  $\text{CuInSe}_2$  films, deposited at a rate of (a, b) 0.1; (c, d) 3.5 and (e, f)  $10 \text{ nm s}^{-1}$ .

TABLE I Electron diffraction data of CuInSe<sub>2</sub> films prepared at different deposition rates

$d_{\text{obs}}$ (nm)			CuInSe <sub>2</sub> (JCPDS 23-208)		InSe (JCPDS 12-118)		Cu <sub>3</sub> Se <sub>2</sub> (JCPDS 19-402)		CuSe (JCPDS)		
	0.1 nm s <sup>-1</sup>	3.5 nm s <sup>-1</sup>	10.0 nm s <sup>-1</sup>	$d$ (nm)	$hkl$	$d$ (nm)	$hkl$	$d$ (nm)	$hkl$	$d$ (nm)	$hkl$
-	-	0.4096	-	-	0.416	400	-	-	-	-	-
-	-	0.3377	-	-	0.338	211	-	-	-	-	-
0.3341	0.335	-	0.334	112	-	-	-	-	-	-	-
-	-	0.3198	-	-	-	-	0.320	200	-	-	-
-	-	0.2844	-	-	-	-	0.2865	210	-	-	-
-	-	0.2465	-	-	0.244	440	-	-	-	-	-
0.2038	0.2044	0.2036	0.204	220	-	-	-	-	-	-	-
-	-	0.1912	-	-	-	-	0.191	301	-	-	-
0.1744	0.1747	0.1744	0.1743	116	-	-	-	-	-	-	-
-	-	0.1674	0.167	224	-	-	-	-	0.1676	202	-
-	-	0.1622	-	-	0.162	432	-	-	0.1622	116	-
-	-	0.1482	0.148	323	-	-	-	-	-	-	-
-	-	0.1410	-	-	-	-	-	-	0.1401	207	-
0.1326	0.1328	-	0.1327	316	-	-	-	-	-	-	-
-	-	0.127	-	-	-	-	0.1278	213	0.1278	212	-
-	0.1179	-	0.1181	424	-	-	-	-	-	-	-
-	-	0.1154	-	-	0.1154	1032	-	-	-	-	-
0.115	-	-	0.1151	501	-	-	-	-	-	-	-
-	0.1114	-	0.1114	336	-	-	-	-	-	-	-
-	-	0.1105	-	-	-	-	-	-	0.1105	218	-

entation, where the (1 1 2) reflecting plane is the predominant plane. This indicates that the film has a fibre texture with the (1 1 2) plane parallel to the film plane. This result accords with those obtained by different evaporation techniques [22, 23]. The lattice parameters  $a_0$  and  $c_0$  of the film, as determined from analysis of the X-ray diffraction data, were found to be  $a_0 = 0.5782$  nm and  $c_0 = 1.1621$  nm, in good agreement with published data [24, 25].

At moderate deposition rates (3.5 nm s<sup>-1</sup>) (Fig. 2b), the film has a polycrystalline structure with a strong (1 1 2) diffraction line and weak (2 2 0), (1 1 6) and (3 3 6) lines of the chalcopyrite tetragonal structure of CuInSe<sub>2</sub>. Fig. 2c shows the multiphase nature obtained in the case of films deposited at higher rates (10 nm s<sup>-1</sup>). In addition to the diffraction lines corresponding to CuInSe<sub>2</sub>, there appears the (1 0 4) and (1 1 0) diffraction lines due to In<sub>2</sub>Se<sub>3</sub>.

Concomitant with the above analysis are the transmission electron micrographs and diffraction patterns shown in Fig. 3a. The electron diffraction data (Table I) showed that the films deposited at low and moderate rates have a single-phase polycrystalline structure corresponding to the chalcopyrite tetragonal structure. At higher rates (10 nm s<sup>-1</sup>) the deposited films showed a multiphase structure containing, in addition to CuInSe<sub>2</sub>, some other phases like InSe, CuSe and Cu<sub>3</sub>Se<sub>2</sub>.

The influence of the film thickness on the orientation of the deposited crystallites is shown in Fig. 4, for thicknesses ranging from 30 to 500 nm. The deposition rate was maintained constant at 0.1 nm s<sup>-1</sup> and the substrate was kept constantly at room temperature. The intensity from the predominant (1 1 2) reflecting plane increases as the film thickness increases. This indicates that the films deposited at low deposition rate (0.1 nm s<sup>-1</sup>) preserve growth through the (1 1 2) plane as their thickness increases.

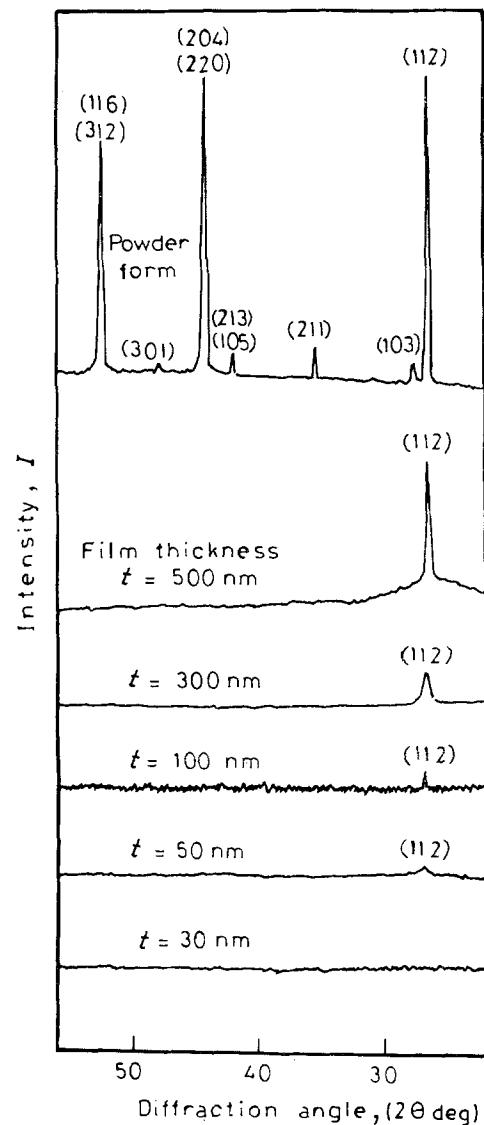


Figure 4 XRD patterns of CuInSe<sub>2</sub> films deposited at a deposition rate of 0.1 nm s<sup>-1</sup> as a function of film thickness.

The film orientation was also found to be affected by post-deposition annealing, Fig. 5 shows the X-ray diffraction pattern for a film deposited at a rate of  $0.1 \text{ nm s}^{-1}$ , followed by annealing at 473 K for 1 h in air, compared with that of the as-deposited films. The intensity of the (1 1 2) line increases and the (2 2 0) and (3 3 2) lines of the chalcopyrite structure also appear. Hence, annealing distorts the orientation of the as-

prepared film and leads to a random polycrystalline structure.

The effect of the substrate temperature on films deposited at a deposition rate of  $3.5 \text{ nm s}^{-1}$ , keeping the substrate temperature at 623 K, is shown in Fig. 6. The (1 1 2) line predominates and the other weak lines nearly disappear, indicating that the film tends to attain a high degree of preferential growth

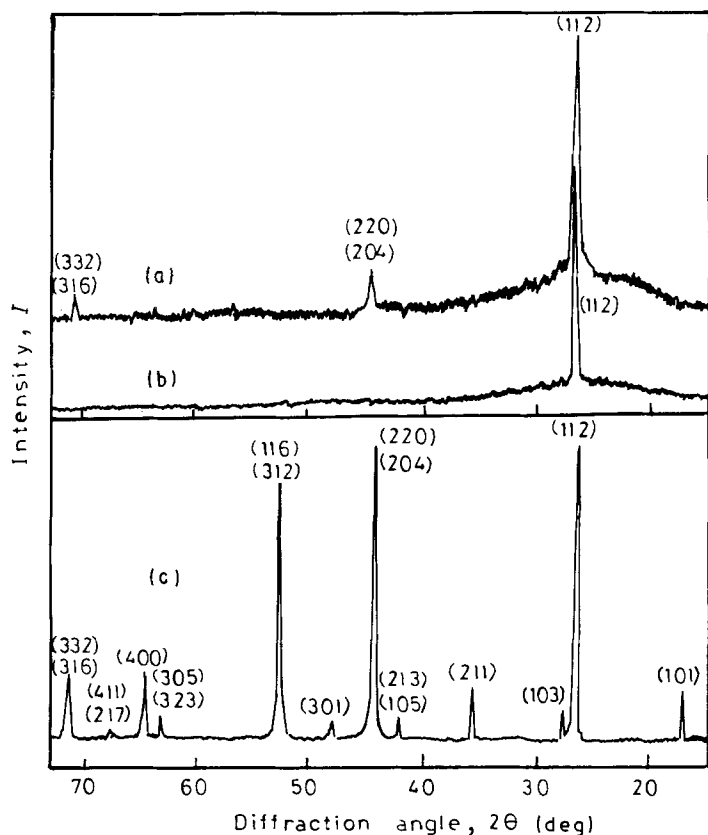


Figure 5 (a) XRD pattern of a  $\text{CuInSe}_2$  film deposited at a rate of  $0.1 \text{ nm s}^{-1}$  after being annealed at 473 K for 1 h, compared with (b) the as-deposited film and (c) the powder pattern.

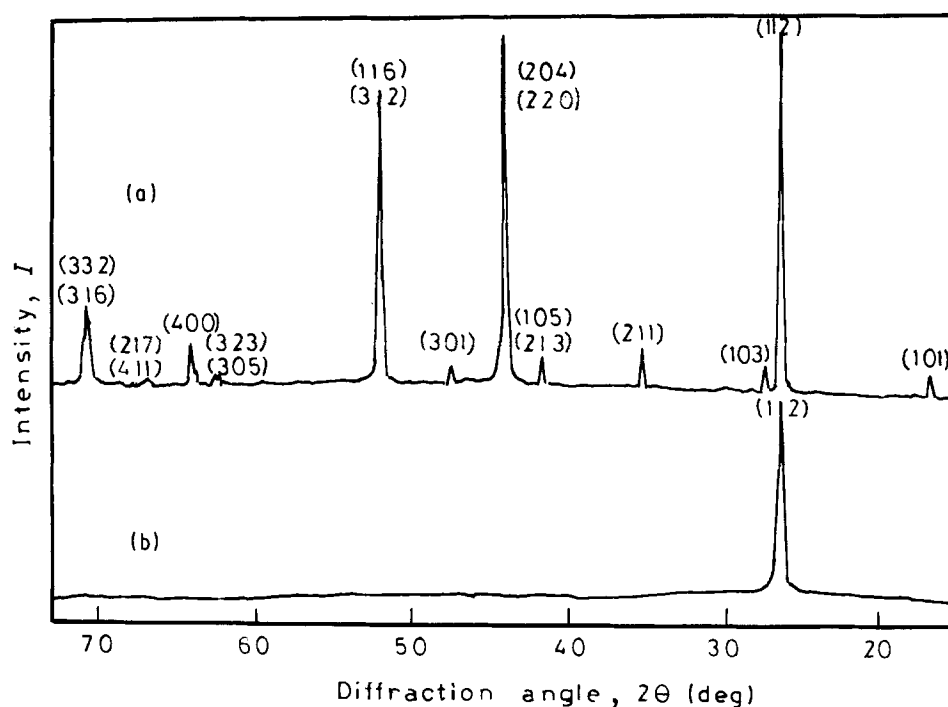


Figure 6 XRD patterns of (a) powder forms and (b)  $\text{CuInSe}_2$  film deposited at a rate of  $3.5 \text{ nm s}^{-1}$  on a heated substrate ( $T_s = 623 \text{ K}$ ).

when deposited on glass substrates kept at elevated temperatures. This result is consistent with that obtained by previous authors [15–18, 21].

Thus, using the single-source evaporation technique, single-phase and nearly stoichiometric  $\text{CuInSe}_2$  films deposited at room temperature on glass substrates could be obtained by controlling the deposition rate below about  $4 \text{ nm s}^{-1}$ .

### 3.2. Electrical resistivity

The temperature dependence of the dark electrical resistivity of  $p$ -type  $\text{CuInSe}_2$  films of different thicknesses, deposited at a rate of  $3.5 \text{ nm s}^{-1}$  on glass substrates kept at room temperature, is typically as shown in Fig. 7. The behaviour follows the relation

$$\rho = \rho_0 \exp(\Delta E/kT)$$

where  $\Delta E = 0.851 \text{ eV}$  is the conductivity activation energy.

Fig. 8 shows the behaviour of another three films deposited at a lower rate ( $0.1 \text{ nm s}^{-1}$ ). Two distinct conduction mechanisms could be deduced with activation energy 0.4 and 1.01 eV, due to extrinsic and intrinsic conduction, respectively.

The variation of the dark electrical resistivity,  $\rho$ , with the substrate temperature  $T_s$ , is shown typically in Fig. 9 for a film of thickness 492 nm, deposited at a

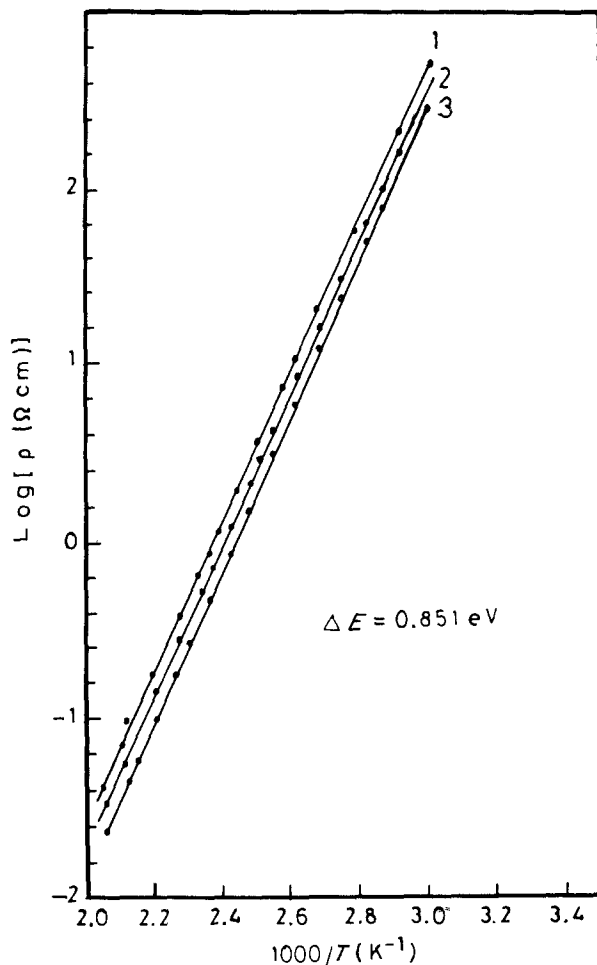


Figure 7 Temperature dependence of the dark electrical resistivity of  $\text{CuInSe}_2$  films of different thickness, deposited at a rate of  $3.5 \text{ nm s}^{-1}$ :  $d$  (nm) = (1) 140, (2) 266, (3) 462.

deposition rate  $3.5 \text{ nm s}^{-1}$ . The resistivity decreases gradually on increasing  $T_s$ , up to 523 K, above which it rises linearly.

Films of the same thickness, 600 nm, were annealed at different temperatures for 1 h in a vacuum. The dependence of  $\rho$  on the annealing temperature  $T_A$  is presented in Fig. 10. The resistivity decreases slightly

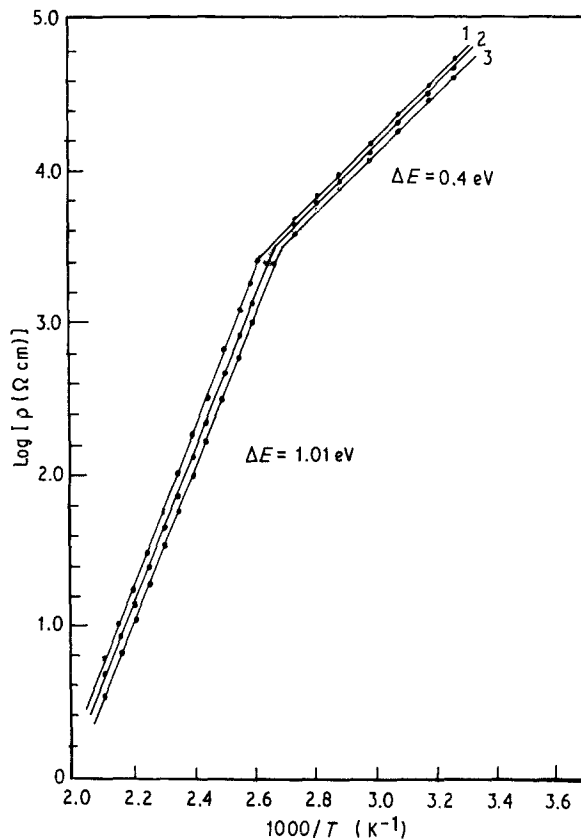


Figure 8 Temperature dependence of the dark electrical resistivity of  $\text{CuInSe}_2$  films deposited at a rate of  $0.1 \text{ nm s}^{-1}$ :  $d$  (nm) = (1) 160, (2) 295, (3) 418.

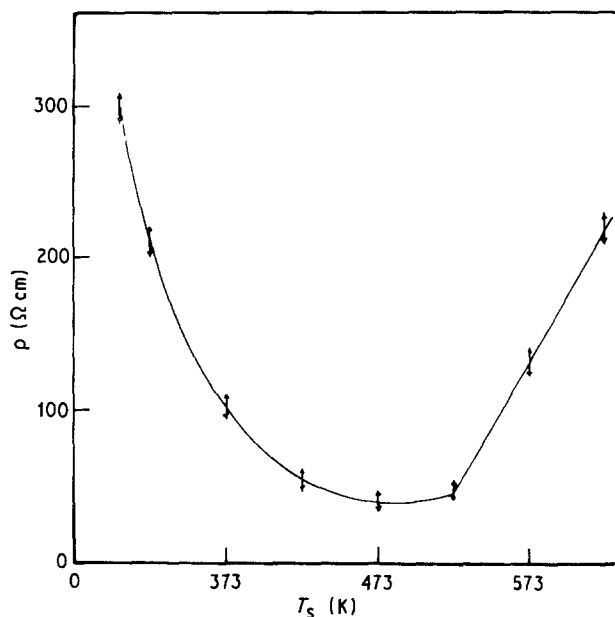


Figure 9 Variation of the resistivity of  $\text{CuInSe}_2$  films (deposition rate  $3.5 \text{ nm s}^{-1}$ , thickness 492 nm) with the substrate temperature,  $T_s$ .

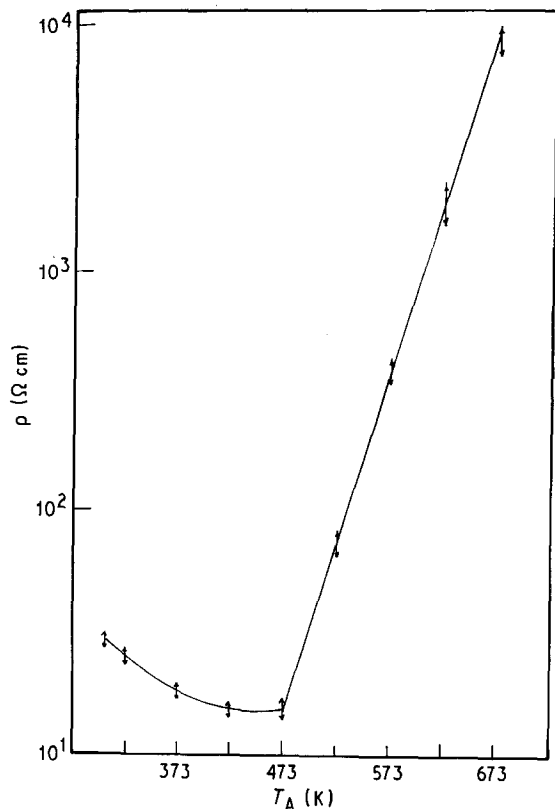


Figure 10 Variation of the resistivity of CuInSe<sub>2</sub> film (600 nm thick) with the annealing temperature,  $T_A$ .

on increasing the annealing temperature from 300 to 473 K. At 473 K the resistivity increases in a linear fashion up to  $T_A = 673$  K (the limit of the range investigated). This may be attributed to the creation of deficient selenium sites during annealing.

## References

1. S. WAGNER, J. L. SHAY, P. MIGLIORATO and H. M. KASPER, *Appl. Phys. Lett.* **25** (1974) 434.
2. L. L. KAZMERSKI, in "Proceedings Third International Conference on Ternary Compounds 1977", Edinburgh, Institute of Physics Conference Series, Vol. 35 (1977) p. 217.

3. E. BUCHER, *Appl. Phys.* **17** (1978) 1.
4. K. HESS, *Nachrichtentech, Electron.* **6** (1979) 185.
5. B. PAMPLIN and R. S. FEIGELSON, *Thin Solid Films* **60** (1979) 141.
6. M. GORSKA, R. BEAULIEU, J. J. LOFERSKI, B. ROSSLER and J. BEALL, *Sol. Energy Mater.* **2** (1980) 343.
7. J. B. MOONEY, R. H. LAMOROEUX and C. W. BATES, SERI PR-8104-TI. (Solar Energy Research Institute, Golden, Colorado, 1980).
8. E. ELLIOTT, R. D. TOMLINSON, J. PARKES and M. J. HAMPSHIRE, *Thin Solid Films* **20** (1974) 525.
9. R. DURNY, A. E. HILL and R. D. TOMLINSON, *ibid.* **69** (1980) L11.
10. L. L. KAZMERSKI, F. R. WHITE, M. S. AYYAGRI, Y. J. JUANG and R. B. PATTERSON, *J. Vac. Sci. Technol.* **14** (1977) 65.
11. L. L. KAZMERSKI, *Thin Solid Films* **57** (1979) 99.
12. R. A. MICHELSON and W. S. CHEN, in Proceedings of 15th IEEE Conference on Photovoltaic Specialists, Orlando, FL, May 12-15, 1981 (IEEE, New York, 1981) p. 800.
13. R. R. ARYA, R. BEAULIEU, M. KWIETNIAK, J. LOFERSKI and L. L. KAZMERSKI, *J. Vac. Sci. Technol.* **20** (1982) 302.
14. B. R. PAMPLIN, *Prog. Cryst. Growth Characteriz.* **1** (1979) 395.
15. R. D. TOMLINSON, D. OMEZI, J. PARKES and M. J. HAMPSHIRE, *Thin Solid Films* **64** (1979) L3.
16. A. F. FRAY and P. LLOYD, *ibid.* **58** (1979) 29.
17. W. HORIG, H. NEUMANN, H. J. HÖBLER and G. KÜHN, *Phys. Status Solidi (b)* **80** (1977) K21.
18. J. PARKES, R. D. TOMLINSON and M. HAMPSHIRE, *J. Solid State Electron.* **16** (1973) 773.
19. H. S. SOLIMAN, M. M. EL-NAHASS, O. JAMJOUR and KH. A. MADY, *J. Mater. Sci. Lett.* **7** (1988) 633.
20. *Idem*, *J. Mater. Sci.* **23** (1988) 4071.
21. W. R. RUNYAM, "Semiconductor Measurements and Instrumentations" (McGraw Hill, Kayakusha Ltd, 1975).
22. B. SCHUMANN, C. GEORGI, A. TEMPEL, G. KÜHN, N. V. NAM, H. NEUMANN and W. HÖRIG, *Thin Solid Films* **52** (1978) 45.
23. L. L. KAZMERSKI, M. S. AYYAGARI, G. H. SANBORN, F. R. WHITE and A. J. MERRILL, *ibid.* **37** (1976) 323.
24. J. PARKES, R. D. TOMLINSON and M. HAMPSHIRE, *J. Appl. Crystallogr.* **6** (1973) 414.
25. H. NEUMANN, E. NOWAK, B. SCHUMANN and G. KÜHN, *Thin Solid Films* **74** (1980) 197.

Received 1 November 1990  
and accepted 25 March 1991